

# STIS UV spectroscopy of early B supergiants in M31<sup>1</sup>

Fabio Bresolin

*Institute for Astronomy, 2680 Woodlawn Drive, Honolulu HI 96822*

bresolin@ifa.hawaii.edu

Rolf-Peter Kudritzki

*Institute for Astronomy, 2680 Woodlawn Drive, Honolulu HI 96822*

kud@ifa.hawaii.edu

Daniel J. Lennon

*Isaac Newton Group, Apartado 321, 38700 Santa Cruz de La Palma, Canary Islands, Spain*

djl@ing.iac.es

Stephen J. Smartt

*Institute of Astronomy, University of Cambridge, Madingley Road, Cambridge CB3 0HA*

sjs@ast.cam.ac.uk

Artemio Herrero

*Instituto de Astrofísica de Canarias, E-38200 La Laguna, Tenerife, Spain*

*Departamento de Astrofísica, Universidad de La Laguna, Avda. Astrofísico Francisco  
Sánchez, s/n, E-38071 La Laguna, Spain*

ahd@ll.iac.es

Miguel A. Urbaneja

*Instituto de Astrofísica de Canarias, E-38200 La Laguna, Tenerife, Spain*

maup@ll.iac.es

---

<sup>1</sup>Based on observations with the NASA/ESA Hubble Space Telescope obtained at the Space Telescope Science Institute, which is operated by the Association of Universities for Research in Astronomy, Incorporated, under NASA contract NAS5-26555.

and

Joachim Puls

*Universitäts-Sternwarte München, Scheinerstrasse 1, 81679, München, Germany*

`uh101aw@usm.uni-muenchen.de`

## ABSTRACT

We analyze STIS spectra in the 1150-1700 Å wavelength range obtained for six early B supergiants in the neighboring galaxy M31. Because of their likely high (nearly solar) abundance, these stars were originally chosen to be directly comparable to their Galactic counterparts, and represent a much-needed addition to our current sample of B-type supergiants, in our efforts to study the dependence of the Wind Momentum-Luminosity Relationship on spectral type and metallicity. As a first step to determine wind momenta we fit the P-Cygni profiles of the resonance lines of N V, Si IV and C IV with standard methods, and derive terminal velocities for all of the STIS targets. From these lines we also derive ionic stellar wind column densities. Our results are compared with those obtained previously in Galactic supergiants, and confirm earlier claims of ‘normal’ wind line intensities and terminal velocities in M31. For half of the sample we find evidence for an enhanced maximum turbulent velocity when compared to Galactic counterparts.

*Subject headings:* galaxies: individual (M31)—galaxies: stellar content—stars: atmospheres—stars: early type—stars: supergiants—stars: winds, outflows

## 1. Introduction

The analysis of mass-loss and stellar winds in early-type supergiants, important *per se* because of the physical insight it provides about the atmospheres of massive stars, has gained momentum in recent years with the realization that it can also provide the basis for the determination of stellar distances, through the dependence of the wind momentum on luminosity. With the work of Puls et al. (1996) and Kudritzki et al. (1999), the Wind Momentum-Luminosity Relationship (WLR) has been established for OBA supergiants in our own Galaxy and in the Magellanic Clouds. The latter paper showed the impact of the differing stellar atmospheric parameters between spectral types on the parameterization of

the WLR. The empirical verification of the predicted dependence of the global properties of stellar winds, and consequently of the WLR, on metallicity has however just begun, because of the considerable observational efforts required (McCarthy et al. 1995, 1997). It is nevertheless reassuring that preliminary results on the massive stellar winds in galaxies even beyond the Local Group agree with the present calibration of the WLR (Bresolin et al. 2001, 2002).

As a next step in the understanding and calibration of the WLR we are carrying out several programs, including the study of OB supergiants of known distances in the Galaxy (Herrero et al. 2001), M33 (Urbaneja et al. 2002) and M31 (this work). This allows us to investigate stellar winds at different metallicities and spectral types, by removing the uncertainty in the distances which afflicts most of the Galactic work (Kudritzki et al. 1999).

In this paper we present our first results on early B (B0-B3) supergiants in the neighboring galaxy M31, obtained from Space Telescope Imaging Spectrograph (STIS) ultraviolet spectra. Given the nearly solar abundance of the observed fields, as inferred from H II region studies (Blair, Kirshner & Chevalier 1982), these stars were originally chosen to be directly comparable to their Galactic counterparts. A comparison of the WLR obtained for two A-type supergiants in M31 with similar objects in the Galaxy has been presented in the work of McCarthy et al. (1997), and by Kudritzki et al. (1999). However, for the purpose of calibrating the WLR, early B supergiants are currently under-represented in the available samples of stars with accurate distances. Moreover, as shown by Kudritzki et al. (1999), changes in the ionization stages of the metals driving the wind around the late O and early B types modify the WLR considerably, and must be thoroughly tracked by gathering more data for stars in this spectral range. For A-type supergiants the wind parameters, including the mass-loss rate and the terminal velocity  $v_\infty$ , can be derived from fits of the  $H\alpha$  line to hydrodynamical models of the expanding atmosphere. However, for OB supergiants, profile fits to the UV P-Cygni resonance lines are required to obtain accurate terminal velocities (Kudritzki & Puls 2000), hence the necessity for HST spectroscopy.

Individual OB supergiants in M31 have been observed previously in the vacuum ultraviolet with the IUE satellite (Bianchi, Hutchings & Massey 1991, and references therein) and with the Faint Object Spectrograph (FOS) on the Hubble Space Telescope (HST; Hutchings et al. 1992, Bianchi et al. 1994). Some of this early work suffered from low spectral resolution and sensitivity, and suggested that the stellar winds of OB supergiants in M31 could be one order of magnitude weaker than in the Galaxy. This result was challenged by Herrero et al. (1994), who concluded from a study of  $H\alpha$  spectra in M31 AB supergiants that their winds should be comparable to those of similar Galactic stars. A reanalysis of FOS data by Bianchi et al. (1994) and Haser et al. (1995) established that mass-loss rates in the studied M31 OB

supergiants are comparable to those found in some of their Galactic counterparts.

The targets for the present investigation are six early B supergiants chosen among the brightest from the surveys of massive stars in M31 by Massey, Armandroff & Conti (1986, CCD *UBV* imaging), Humphreys, Massey & Freedman (1990) and Massey et al. (1995, optical spectroscopy). The nomenclature adopted here for the parent OB associations (see Table 1) is the one introduced by van den Bergh (1964). One of the supergiants lies in Baade’s Field IV (Baade & Swope 1963), within the boundaries of van den Bergh’s association OB184, one of the outermost associations in the disk of M31, 96’ (22 Kpc) southwest of the nucleus. This star is indicated as IV-B59 in Table 1, and is one of the three early-type supergiants included in the study of Humphreys (1979). Of the remaining stars, two are found in OB78 (=NGC 206), and one in OB48, both among the richest OB associations in M31, located in the most actively star forming annular region, between 9 and 15 Kpc, identified by van den Bergh (1964). The last two objects are part of OB8 and OB10, at the smallest galactocentric distance ( $\sim 6$  Kpc) in the sample considered here.

High resolution optical spectra of all the STIS targets have been obtained by us with the William Herschel Telescope (WHT) on La Palma and with the Keck I telescope. The analysis of the WHT spectra are presented in a companion paper (Trundle et al. 2002), deriving stellar parameters and photospheric abundances. A future analysis of the complete data set will be achieved in a unified, consistent approach to further yield mass-loss rates and a full test of the WLR for the M31 galaxy. We also note that previous optical spectroscopic work on individual B- and A-type M31 supergiants has been carried out by Herrero et al. (1994, the star OB78-478 is in common with our present sample), McCarthy et al. (1997), Venn et al. (2000) and Smartt et al. (2001, star OB10-64 in common with current work).

In this paper we concentrate on the measurement of the terminal velocities from the analysis of the main resonance lines in the UV spectrum. We describe the STIS observations of the six B supergiants in M31 in § 2, and the method used to derive the terminal velocities in § 3. We comment on the individual stars in § 4, and we briefly discuss our results in § 5.

## 2. Observations

The data were collected with STIS aboard HST (Woodgate et al. 1998, Kimble et al. 1998), using the 0.2 arcsec-wide slit, combined with the G140L grating and the FUV MAMA detector. This setup delivered spectra in the 1150-1700 Å wavelength range, at  $R \sim 1000$  resolution. Total exposure times and observing dates are summarized in Table 1, together with the main observational data for the six M31 supergiants. Magnitudes are from CCD

photometry (Massey et al. 1995), except in the case of IV-B59 (photoelectric measurement by Humphreys 1979). The spectral types, initially drawn from Massey et al. (1995, = M95 in Table 1), and from Humphreys (1979) for IV-B59, have been revised from the new optical spectra obtained at the WHT (Trundle et al. 2002, = T02). For the following analysis of the UV spectra we adopted the radial velocities determined from our optical spectra, with corresponding uncertainties of  $10\text{--}20\text{ km s}^{-1}$ . WFPC2 images of some of our fields reveal that OB 78-159 is a composite object, consisting of at least three stars. Multi-color WFPC2 images for OB 48-358 and OB 78-478 show them to be single objects at the HST resolution, while the STIS acquisition images for the remaining three targets also indicate they are single.

The pipeline-processed extracted spectra were averaged and rectified, using a low-order polynomial to fit regions of the continuum relatively free of stellar features, as indicated by stellar atmosphere models (e.g., Leitherer et al. 2001). Although the procedure is made uncertain by heavy blocking from metal lines (mostly iron), especially redwards of C IV  $\lambda 1550$ , and by interstellar Ly  $\alpha$  absorption, the following results pertaining to the analysis of the resonance wind lines remain virtually unaffected.

Rectified spectra are displayed in Fig. 1. The wavelength region covered includes some of the most important diagnostics of stellar winds, i.e., the doublets N V  $\lambda\lambda 1239, 1243$  (hereafter abbreviated as N V  $\lambda 1240$ ), Si IV  $\lambda\lambda 1394, 1403$  (Si IV  $\lambda 1400$ ) and C IV  $\lambda\lambda 1548, 1551$  (C IV  $\lambda 1550$ ). The P-Cygni profiles observed in all these lines are consistent with the expected profiles for early B-type supergiants (Walborn & Nichols-Bohlin 1987), with a decreasing wind effect as one goes from B0 to B2 supergiants. N V is virtually absent in the later type star, IV-B59. Several photospheric lines can be identified, including C III  $\lambda 1176$ , O IV  $\lambda 1339, 1343$  and He II  $\lambda 1640$ . The displacement towards short wavelengths of the C III  $\lambda 1176$  blend observed for the earlier type stars (OB 78-159, OB 10-64 and OB 48-358) is consistent with the wind effect seen in O4-B0 supergiants, and which quickly declines after the B0.5 Ia class (Snow & Morton 1976).

The presence of several absorption lines due to Fe V and Fe IV is responsible for the continuum depression at wavelengths longer than  $1400\text{ \AA}$ . Moreover, prominent interstellar lines are visible throughout the spectra, originating from singly ionized Si (e.g., Si II  $\lambda 1193$ ,  $\lambda 1260$  and  $\lambda 1527$ ), and additional metals, as identified in Fig. 1. For the stars with a higher radial velocity ( $v_{rad} \simeq 500\text{ km s}^{-1}$ ) these features are generally broader, because of the resulting larger separation in wavelength between the M31 and the Galactic contribution.

### 3. Analysis of the resonance lines

For the analysis of the resonance lines and the determination of the terminal velocities we used the method described by Haser (1995, see also Haser et al. 1995). This is based on the SEI-method developed by Lamers, Cerruti-Sola & Perinotto (1987, see also Hamann 1981) for the calculation of line profiles in stellar winds, and which has been adopted in subsequent investigations of the UV line profiles of massive stars (Groenewegen & Lamers 1989, Lamers et al. 1999, Herrero et al. 2001). Here we briefly describe the formalism adopted in this work, for further details the reader is referred to the papers cited above. The wind flow is described by a  $\beta$ -law:

$$w(x) = (1 - b/x)^\beta \quad b = (1 - w_{min}^{1/\beta})$$

where  $x = r/R_*$  is the radial coordinate normalized to the stellar radius,  $w(x) = v(x)/v_\infty$  is the flow velocity normalized to the terminal velocity, and  $w_{min} = w(x = 1)$  is considered fixed at 0.01. Following Haser (1995), a wind ‘turbulent’ velocity increasing with radius is assumed:

$$v_{turb} = a_t v(r) + b_t \quad a_t = \frac{v_{ta} - v_{ti}}{1 - v_{min}} \quad b_t = v_{ta} - a_t,$$

with  $v_{ti}$  and  $v_{ta}$  the minimum and maximum turbulent velocities, reached at  $w = w_{min}$  and  $w = w_{max} = 1$ , respectively.

To account for the contamination of the observed line profiles by photospheric lines we used IUE spectra of B-type main sequence stars having weak winds and small projected rotational velocities. The calculated line profiles, once their resolution was degraded to match the resolution of the STIS spectra, were then directly comparable to the observed ones. Our adopted best fits for the N V, Si IV and C IV doublets are displayed, along with the observed line profiles, in Fig. 2 and 3. Even though the quality of the fit to the emission peaks, as well as to the central part of the line profiles, depends on the chosen photospheric templates, the derived terminal velocities are quite insensitive to this choice. Some additional caution had to be taken when fitting the profiles, because of the contamination from instrumentally broadened interstellar lines and because of the depression of the pseudocontinuum created by strong metal line blocking on the blue side of C IV  $\lambda$  1550. Stellar rotation is not expected to play a major role in our results, since typical rotational velocities for early B supergiants are  $\sim 50\text{--}80 \text{ km s}^{-1}$ .

There is in general a good agreement in the terminal velocities derived from the different resonance lines. Their mean values are summarized in Table 2 (column 8, with errors given in brackets), together with the range in maximum turbulent velocity found to be acceptable

for the fits (column 9), and the exponent  $\beta$  of the wind parameterization (column 10). The uncertainty in the terminal velocities is of order 50 to 100 km s<sup>-1</sup>, as estimated from model fits obtained varying  $v_{ta}$  and  $v_{\infty}$  in combination. Concerning the maximum turbulent velocity, for half of the sample its largest value in the estimated range of validity is comparable to the spectral resolution of the data (approximately 250 km s<sup>-1</sup>), so that secure inferences about the  $v_{ta}/v_{\infty}$  ratio cannot be drawn. We conclude that these data are not inconsistent with previous studies of Galactic supergiants, for which  $v_{ta}/v_{\infty} = 0.08 - 0.15$  (Groenewegen & Lamers 1989, Haser 1995, Herrero et al. 2001). For the remaining objects (OB 78-159, OB 10-64 and OB 8-17), on the other hand, we find some evidence for an enhanced  $v_{ta}$ , in particular large turbulent velocities ( $v_{ta}/v_{\infty} \simeq 0.20 - 0.30$ , with  $v_{ta}$  in excess of the spectral resolution) seem to be required in order to explain both the blue slope and the width of the resonance line profiles (broader than those found in spectra of Galactic supergiants observed with IUE and degraded to STIS resolution). This result is in agreement with a similar finding in a sample of early B supergiants in M33 (mean  $v_{ta}/v_{\infty} = 0.25$ ) studied by Urbaneja et al. (2002).

Column densities (in cm<sup>-2</sup>) for the three ions reported in Table 2 (columns 11-13) were calculated as in Haser (1995, see also Herrero et al. 2001), from the integration of the line strengths between  $w = 0.2$  and  $w = 1.0$ . In Table 2, we have adopted a distance to M31 of 783 Kpc (Holland 1998) for deriving radial galactocentric distances  $R$  (column 2) and absolute magnitudes  $M_V$  (column 5).

### 3.1. HI column densities

The column density of neutral hydrogen atoms along the line of sight,  $N(H I)$ , was estimated from the observed interstellar medium Ly  $\alpha$  absorption, assuming a pure damping profile for this line (Bohlin 1975). The profiles for the adopted column densities are illustrated in Fig. 4 (dashed lines), together with the profiles obtained by varying  $N(H I)$  by  $\pm 0.1$  dex (dotted lines), our estimated uncertainty from the comparison of damping profiles having different column densities with the observed ones. In the fits more weight was given to the red part of the line wings, since the blue part is more heavily affected by absorption features. A look at Fig. 4 shows that for the two stars for which we derive the largest  $N(H I)$  (OB 78-478 and IV-B59) the fits are also the most uncertain. We have verified that the stellar contribution to the Ly  $\alpha$  line wings is minimal, and does not affect the estimated  $N(H I)$  in a significant way.

The resulting total column densities are given in column 6 of Table 2, while column 4 contains the color excess  $E(B - V)$ , taken as the average for a given OB association, from

Massey et al. (1995) and Humphreys (1979).  $E(B - V)$  values for the single stars are also given by these authors, and are within 0.06 mag (of the same order as the typical uncertainty on the measured colors) of the parent association average, which we prefer in this case in order to avoid errors from possible spectral type misclassifications. To estimate the gas-to-dust ratio as derived from these measurements, we first removed the Galactic foreground contribution, taking the color excess in the direction of M31 from Schlegel, Finkbeiner & Davis (1998),  $E(B - V)_{Gal} = 0.06$  mag, and the average gas-to-dust ratio from Savage & Mathis (1979),  $[N(HI)/E(B - V)]_{Gal} = 5.0 \times 10^{21} \text{ cm}^{-2} \text{ mag}^{-1}$ . The resulting  $N(HI)/E(B - V)_0$ , intrinsic to M31, is given in column 7, with corresponding uncertainties in brackets, assuming a 0.04 mag error in the color index.

The weighted mean ratio,  $N(HI)/E(B - V)_0 = 5.1 (\pm 1.3) \times 10^{21} \text{ cm}^{-2} \text{ mag}^{-1}$ , compares well with the Galactic one, and with previous determinations for M31. Using globular clusters as tracers of reddening, Bajaja & Gergely (1977) found a radial dependence of the M31 gas-to-dust ratio, averaging  $3.3 \times 10^{21} \text{ cm}^{-2} \text{ mag}^{-1}$ , while van den Bergh (1975) found a value similar to the Galactic one (see also Braun & Walterbos 1992, who used the Balmer decrement of ionized gas as a measure of reddening). Higher values have been recently reported by Cuillandre et al. (2001), ranging between  $N(HI)/E(B - V)_0 = 1.1 \times 10^{22} \text{ cm}^{-2} \text{ mag}^{-1}$  (using background galaxies seen through the disk of M31) and  $1.45 \times 10^{22} \text{ cm}^{-2} \text{ mag}^{-1}$  (from M31 stars) in an outer field of M31.

#### 4. Comments on individual supergiants

In order to compare the UV spectral properties of our sample of M31 stars with counterparts observed in the Galaxy, we show in Fig. 5 and 6 our rectified STIS spectra, together with selected Galactic OB supergiant spectra from the atlases of Walborn, Nichols-Bohlin & Panek (1985) and Walborn, Parker & Nichols (1995). The three top panels of Fig. 5 illustrate the three B0Ia stars in M31, while the remaining panels in this figure show IUE spectra of Galactic supergiants ranging in spectral type from O9.7 to B0.5, degraded to  $1.5 \text{ \AA}$  resolution. In a similar fashion, in Fig. 6 the three later type supergiants in M31 are compared to B1-B3Ia Galactic stars. In the following we discuss the comparison on a star-by-star basis, and briefly comment on the results obtained from the wind analysis of the individual M31 supergiants.

*OB 78-159:* Low resolution spectra of this star, as well as of OB 8-17, OB 10-64 and OB 48-358, obtained with HST/FOS, were described qualitatively by Bianchi, Hutchings & Massey (1996), who pointed out the general similarity between the UV spectra of the M31 supergiants and Galactic counterparts of the same optical spectral type. The low spectral



resolution of their data, however, did not allow accurate quantitative measurements of the terminal velocities. The STIS acquisition images show two fainter neighboring stars, the closest being  $\sim 0.3$  arcsec from the blue supergiant along the spatial direction in the spectra, and which does not interfere with the extracted spectrum of OB 78-159. However, in future studies the luminosity inferred from the ground-based apparent magnitude would have to be corrected using high spatial resolution photometry with HST. The UV spectrum more closely resembles that of the Galactic B0.5 Ia template ( $\kappa$  Ori) rather than the B0 Ia template ( $\epsilon$  Ori). It is quite possible that the optical classification is compromised by the contamination from the neighboring stars. The measured value  $v_\infty = 1200 \text{ km s}^{-1}$  for the terminal velocity is also below the average for Galactic B0 supergiants ( $1550 \text{ km s}^{-1}$ ), although still within the range for B0 Ia stars (Prinja, Barlow & Howarth 1990, Howarth et al. 1997), and more in agreement with the average  $v_\infty = 1380 \text{ km s}^{-1}$  found for Galactic B0.5 Ia stars (Haser 1995).

*OB 10-64:* A partial analysis of our STIS spectrum was included in the work of Smartt et al. (2001). We have slightly revised the terminal velocity downwards given there from  $v_\infty = 1650 \text{ km s}^{-1}$  to  $1600 \text{ km s}^{-1}$ , in order to obtain an agreement between the three lines for which we attempted a profile fit, while the earlier result was more weighted to the C IV  $\lambda 1550$  line. This is the only supergiant for which we currently have a mass-loss determination,  $\dot{M} = 1.6 \times 10^{-6} M_\odot \text{ yr}^{-1}$ , from the analysis of the H $\alpha$  line (Smartt et al. 2001). The Si IV wind line profile in this star is more typical of O9-O9.7Iab supergiants rather than B0 Ia, as can be seen in Fig. 5. The same can be said for the spectrum of OB 48-358. Within the uncertainties these two stars have the same terminal velocity, which is considerably larger ( $\sim 35\%$ ) than the one measured in the other B0 Ia star, OB 78-159.

*OB 48-358:* See comments for OB 10-64.

*OB 8-17:* The star is classified as B1 Ia by Trundle et al. (2002), and its UV spectrum well matches that of B0.7 Ia or B1 Ia Galactic supergiants. The wind line N V  $\lambda 1240$  in general becomes weaker than observed here in Galactic supergiants later than B1 Ia, and also the other resonance lines in the spectrum of OB 8-17 show a good match with HD 148688 (B1 Ia), as illustrated in Fig. 6. Indications for a match with the optical classification comes also from C III  $\lambda 1175$ , which is blueshifted. The terminal velocity well agrees with that of typical B1 Ia supergiants in the Galaxy.

*OB 78-478:* Massey, Hutchings & Bianchi (1985) first discussed IUE spectra of this star in the OB association NGC 206, later reanalyzed by Bianchi, Hutchings & Massey (1991). The appearance of the STIS spectrum is in agreement with Galactic UV spectra corresponding to its optical spectral type (B1.5 Ia). The terminal velocity  $v_\infty = 550 \text{ km s}^{-1}$  also agrees with the typical value found for Galactic B1.5 supergiants.

*IV-B59*: This is the coolest star in the sample, with a UV spectrum consistent with the spectra of Galactic supergiants of type B2.5-B4 Ia-Ib. Earlier or later types are ruled out by the strength of both the C IV and Si IV lines. This is in agreement with the range in spectral type found from the optical spectra. Humphreys (1979) classified this star as B2Iae (with H $\beta$  and H $\gamma$  filled in), while more recent WHT spectra suggest a range between B2Ib and B5Iab (Smartt et al. 2002). Wind effects on the line profiles are rather weak, and an absorption component on the blue side of the line profiles increases the uncertainty in  $v_\infty$ . The model fit to the Si IV doublet shown in Fig. 3 was calculated without photospheric contribution, because of the likely metallicity mismatch with the Galactic template. Our result  $v_\infty = 630 \text{ km s}^{-1}$  is in agreement with the study of Galactic supergiants by Haser (1995), who found average terminal velocities between 750 and 570  $\text{km s}^{-1}$  in the B2-B3 spectral type range. Individual values between 405 and 830  $\text{km s}^{-1}$  were found at B3 by Prinja, Barlow & Howarth (1990).

## 5. Discussion and conclusions

In our previous work on the UV spectra of B supergiants in the Galactic Cyg OB2 association (Herrero et al. 2001) we were able to use some of the stellar parameters derived from optical spectra, together with the known Galactic WLR (Puls et al. 1996) and an assumed set of abundances, to estimate mass-loss rates and mean ionization fractions. Given the uncertainties in abundances and ionization fractions for the current sample of B supergiants in M31, we defer a more complete analysis to a future paper, where we will analyze WHT and Keck optical spectra in order to measure the stellar parameters, and in addition the mass-loss rates from fits to the H $\alpha$  line profiles. When combined with the terminal velocities obtained in this work, we will be able to derive a WLR for early B supergiants in M31. In the following we will make some qualitative comparisons with Galactic supergiants, and draw some preliminary conclusions.

The abundance gradient in M31 has been characterized by relatively few studies of H II region emission lines (e.g., Dennefeld & Kunth 1981; Blair, Kirshner & Chevalier 1982; Galarza, Walterbos & Braun 1999). The large angular extent of the galaxy and the general faintness of the H II regions has precluded more extensive and complete spectroscopic surveys of the gaseous abundances. Moreover, the low excitation of the nebulae implies that the auroral lines necessary to determine the electron temperature remain undetected, with the consequence that empirical strong line methods must be used to estimate the abundances. A recent reanalysis of the available H II region abundances, based on the empirical abundance calibration of McGaugh (1991), has been presented by Smartt et al. (2001). The resulting

oxygen abundance gradient would imply a range between  $12 + \log(O/H) = 8.9$  (at the radial distance of OB 8-17 and OB 10-64) and 8.6 (IV-B59) for the current sample of B-type supergiants, i.e., between a roughly solar abundance and a 0.3 dex lower value. On the other hand, the scant data available from direct stellar abundance determinations (Smartt et al. 2001, Venn et al. 2000) is consistent with a flat gradient between 5 and 20 Kpc, with a value close to that found in the Galactic solar neighborhood ( $12 + \log(O/H) = 8.7 \pm 0.1$ , from the mean NLTE value of Rolleston et al. 2000). The two methods (nebular vs. stellar) of abundance determination might not be in disagreement, given the large scatter in the derived nebular  $O/H$  ratio at a given radial position, and the small number of stellar data available. However, the result obtained for OB 10-64 by Smartt et al. (2001,  $12 + \log(O/H) = 8.7$ ) is well below the value obtained from H II regions at a similar galactocentric distance.

A detailed abundance study of the B supergiants observed with HST is beyond the scope of the present paper, and is addressed in the companion paper by Trundle et al. (2002). Therefore here we directly compare the UV spectra of B-type supergiants in M31 with stars of similar spectral type in the Galaxy. Any large discrepancies would immediately reveal differences in the stellar abundances and/or the wind properties. In Fig. 7 the spectra of two B0Ia supergiants (OB 10-64 and OB 48-358) are shown superimposed on the IUE spectrum of the Galactic O9.7 Iab star HD 149038. The latter was retrieved from the IUE archive at STScI and rectified in the same way as done for the M31 stars. There is an overall excellent agreement between the three spectra. In particular, we note a good match in the spectral regions most affected by metal (mostly iron) lines, between 1410 and 1500 Å, and at wavelengths redwards of C IV  $\lambda$  1550. The Si IV  $\lambda$  1400 and C IV  $\lambda$  1550 wind line profiles are also very similar in the M31 and Galactic supergiants, with nearly the same terminal velocities and peak intensities. A second example is illustrated in Fig. 8, where the UV spectra of IV-B59 and  $\kappa$  Cru (B3Ia) are compared. In this case a slight underabundance is suggested in the spectrum of the M31 star, which would be in agreement with its large galactocentric distance (22 Kpc). The WHT spectra of IV-B59 are not of high enough quality for the accurate measurement of metal lines, hence an abundance analysis of this star is not presented in Trundle et al. (2002). The H II region BA 500 (Baade & Arp 1964) lies only 10'' east of IV-B59, and its emission line fluxes were measured by Dennefeld & Kunth (1981). Applying to their measurements the analytical expression given by Kobulnicky, Kennicutt & Pizagno (1999) for the determination of empirical abundances, based on the strength of the [O II]  $\lambda$  3727 and [O III]  $\lambda\lambda$  4959,5007 lines, and on the McGaugh (1991) photoionization models, we obtain  $12 + \log(O/H) = 8.53$ , which is approximately 2/3 of the oxygen abundance in the solar neighborhood. However, the F5 supergiant A-207, also located in Baade's Field IV, has been found to have a roughly solar abundance by Venn et al. (2000). More detailed abundance studies of individual BA supergiants in M31 are clearly needed to clarify

the issue of the abundance gradient in this galaxy.

Similar qualitative comparisons have been shown by Bianchi, Hutchings & Massey (1996, see also Bianchi et al. 1994, Haser et al. 1995), who compared the UV spectral appearance of M31 and M33 early B supergiants with Galactic and LMC ones. The effects of the lower metal abundance were clearly seen in the M33 stars (see also Urbaneja et al. 2002), with weaker absorption in the Si IV and C IV lines, and in the metal lines in general, in a similar fashion to what is observed in the LMC stars. On the other hand, in the case of M31 their results are comparable to those shown in Fig. 7-8.

Our data (see Table 2), together with previous reliable determinations of terminal velocities in M31 supergiants (Bianchi et al. 1994; Haser et al. 1995; Bianchi, Hutchings & Massey 1996), support the idea that the winds in M31 stars are comparable to those observed in the Galaxy. This is also supported by the H $\alpha$  spectra studied by Herrero et al. (1994) and by the differential analysis of the optical spectra by Trundle et al. (2002), which indicates that four of the stars have very similar abundances to those derived in B-type supergiants in our Galaxy within 1-2 Kpc of the Sun’s position. The oxygen abundances derived are listed for reference in column 3 of Table 2. The absolute value for OB 8-17 appears significantly lower than the others at 8.4 dex. However, a differential abundance analysis with two solar neighbourhood supergiants indicates that OB 8-17 has a very similar oxygen abundance compared to these Milky Way stars. This is also supported by a comparison of the UV spectrum of this object with that of its Galactic counterpart, HD 148688.

Although in one instance the measured  $v_\infty$  is well below the mean Galactic value for the given spectral type, all available data lie within the range observed for Galactic stars, and are therefore consistent with the expected scatter in M31. This is summarized in Fig. 9, where the Galactic data have been taken from the compilations of terminal velocities of O and B supergiants by Haser (1995) and Howarth et al. (1997). A similar conclusion was reached by Bianchi, Hutchings & Massey (1996), although their terminal velocities are in general less accurate than the ones measured with STIS, because of the lower resolution of some of their data.

Our next step will be to add the information from the high-resolution optical spectra, in order to derive wind momenta for the supergiants studied here. This will allow us to provide better constraints on the WLR for early B supergiants of solar abundance.

This work was supported in part by the German DLR under grant 50 OR 9909 2. AH and MAU thank the Spanish MCyT for financial support under project AYA2001-0436.

## REFERENCES

- Baade, W., & Arp, H.C. 1964, ApJ, 139, 1027
- Baade, W., & Swope, H.H. 1963, AJ, 68, 435
- Bajaja, E., & Gergely, T.E. 1977, A&A, 61, 229
- Bianchi, L., Hutchings, J.B., & Massey, P. 1996, AJ, 111, 2303
- Bianchi, L., Lamers, H.J.G.L.M., Hutchings, J.B., Massey, P., Kudritzki, R., Herrero, A., & Lennon, D.J. 1994, A&A, 292, 213
- Bianchi, L., Hutchings, J.B., & Massey, P. 1991, A&A, 249, 14
- Blair, W.P., Kirshner, R.P., & Chevalier, R.A. 1982, ApJ, 254, 50
- Bohlin, R.C. 1975, ApJ, 200, 402
- Braun, R., & Walterbos, R.A.M. 1992, ApJ, 386, 120
- Bresolin, F., Gieren, W., Kudritzki, R.-P., Pietrzyński, G., & Przybilla, N. 2002, ApJ, 567, 277
- Bresolin, F., Kudritzki, R.-P., Mendez, R.H., & Przybilla, N. 2001, ApJ, 548, L159
- Cuillandre, J.-C., Lequeux, J., Allen, R.J., Mellier, Y., & Bertin, E. 2001, ApJ, 554, 190
- Dennefeld, M., & Kunth, D. 1981, AJ, 86, 989
- Galarza, V.C., Walterbos, R.A.M., & Braun, R. 1999, AJ, 118, 2775
- Groenewegen, M.A.T., & Lamers, H.J.G.L.M. 1989, A&AS, 79, 359
- Hamann, W.-R. 1981, A&A, 93, 353
- Haser, S.M. 1995, Ph.D. Thesis, Universitäts-Sternwarte der Ludwig-Maximillan Universität, München
- Haser, S.M., Lennon, D.J., Kudritzki, R.-P., Puls, J., Pauldrach, A.W.A., Bianchi, L., & Hutchings, J.B. 1995, A&A, 295, 136
- Herrero, A., Puls, J., Corral, L.J., Kudritzki, R.-P., & Villamariz, M.R. 2001, A&A, 366, 623

- Herrero, A., Lennon, D.J., Vilchez, J.M., Kudritzki, R.P. & Humphreys, R.H., 1994, A&A, 287, 885
- Holland, S. 1998, AJ, 115, 1916
- Howarth, I.D., Siebert, K.W., Hussain, G.A.J., & Prinja, R.K. 1997, MNRAS, 284, 265
- Humphreys, R.M., Massey, P., & Freedman, W.L. 1990, AJ, 99, 84
- Humphreys, R.M. 1979, ApJ, 234, 854
- Hutchings, J.B., Bianchi, L., Lamers, H.J.G.L.M., Massey, P., & Morris, S.C. 1992, ApJ, 400, L35
- Hutchings, J.B., Massey, P., & Bianchi, L. 1987, ApJ, 322, L79
- Kimble, R.A., et al. 1998, ApJ, 492, L83
- Kobulnicky, H.A., Kennicutt, R.C., & Pizagno, J.L. 1999, ApJ, 514, 544
- Kudritzki, R.-P., & Puls, J. 2000, ARA&A, 38, 613
- Kudritzki, R.P., Puls, J., Lennon, D.J., Venn, K.A., Reetz, J., Najarro, F., McCarthy, J.K., & Herrero, A. 1999, A&A, 350, 970
- Lamers, H.J.G.L.M., Haser, S., de Koter, A., & Leitherer, C. 1999, ApJ, 516, 872
- Lamers, H.J.G.L.M., Cerruti-Sola, M., & Perinotto, M. 1987, ApJ, 314, 726
- Leitherer, C., Leao, J.R.S., Heckman, T.M., Lennon, D.J., Pettini, M., & Robert, C. 2001, ApJ, 550, 724
- Massey, P., Armandroff, T.E., Pyke, R., Patel, K., & Wilson, C.D. 1995, AJ, 110, 2715
- Massey, P., Armandroff, T.E., & Conti, P.S. 1986, AJ, 92, 1303
- Massey, P., Hutchings, J.B., & Bianchi, L. 1985, AJ, 90, 2239
- McCarthy, J.K., Kudritzki, R.-P., Lennon, D.J., Venn, K.A., & Puls, J. 1997, ApJ, 482, 757
- McCarthy, J.K., Lennon, D.J., Venn, K.A., Kudritzki, R.-P., Puls, J., & Najarro, F. 1995, ApJ, 455, L135
- McGaugh, S.S. 1991, ApJ, 380, 140
- Prinja, R.K., Barlow, M.J., & Howarth, I.D. 1990, ApJ, 361, 607

- Puls, J., Kudritzki, R.-P., Herrero, A., Pauldrach, A.W.A., Haser, S.M., Lennon, D.J., Gabler, R., Voels, S.A., Vilchez, J.M., Wachter, S., & Feldmeier, A. 1996, *A&A*, 305, 171
- Rolleston, W.R.J., Smartt, S.J., Dufton, P.L., & Ryans, R.S.I. 2000, *A&A*, 363, 537
- Savage, B.D., & Mathis, J.S. 1979, *ARA&A*, 17, 73
- Schlegel, D.J., Finkbeiner, D.P., & Davis, M. 1998, *ApJ*, 500, 525
- Shaver, P.A., McGee, R.X., Newton, L.M., Danks, A.C., & Pottasch, S.R. 1983, *MNRAS*, 204, 53
- Smartt, S.J., et al. 2002, in preparation
- Smartt, S.J., Crowther, P.A., Dufton, P.L., Lennon, D.J., Kudritzki, R.P., Herrero, A., McCarthy, J.K., & Bresolin, F. 2001, *MNRAS*, 325, 257
- Snow, T.P., & Morton, D.C. 1976, *ApJS*, 32, 429
- Trundle, C., Dufton, P.L., Lennon, D.J., Smartt, S.J., & Urbaneja, M.A. 2002, *A&A*, submitted
- Urbaneja, M.A., Herrero, A., Kudritzki, R.-P., Bresolin, F., Corral, L.J., & Puls, J. 2002, *A&A*, in press
- van den Bergh, S. 1975, *A&A*, 41, 53
- van den Bergh, S. 1964, *ApJS*, 9, 65
- Venn, K.A., McCarthy, J.K., Lennon, D.J., Przybilla, N., Kudritzki, R.P., & Lemke, M. 2000, *ApJ*, 541, 610
- Walborn, N.R., Parker, J.W., & Nichols, J.S. 1995, *International Ultraviolet Explorer Atlas of B-Type Spectra From 1200 to 1900 Å*, Nasa Ref. Publ. 1363
- Walborn, N.R., & Nichols-Bohlin, J. 1987, *PASP*, 99, 40
- Walborn, N.R., Nichols-Bohlin, J., & Panek, R.J. 1985, *International Ultraviolet Explorer Atlas of O-Type Spectra From 1200 to 1900 Å*, Nasa Ref. Publ. 1155
- Woodgate, B.E., et al. 1998, *PASP*, 110, 1183

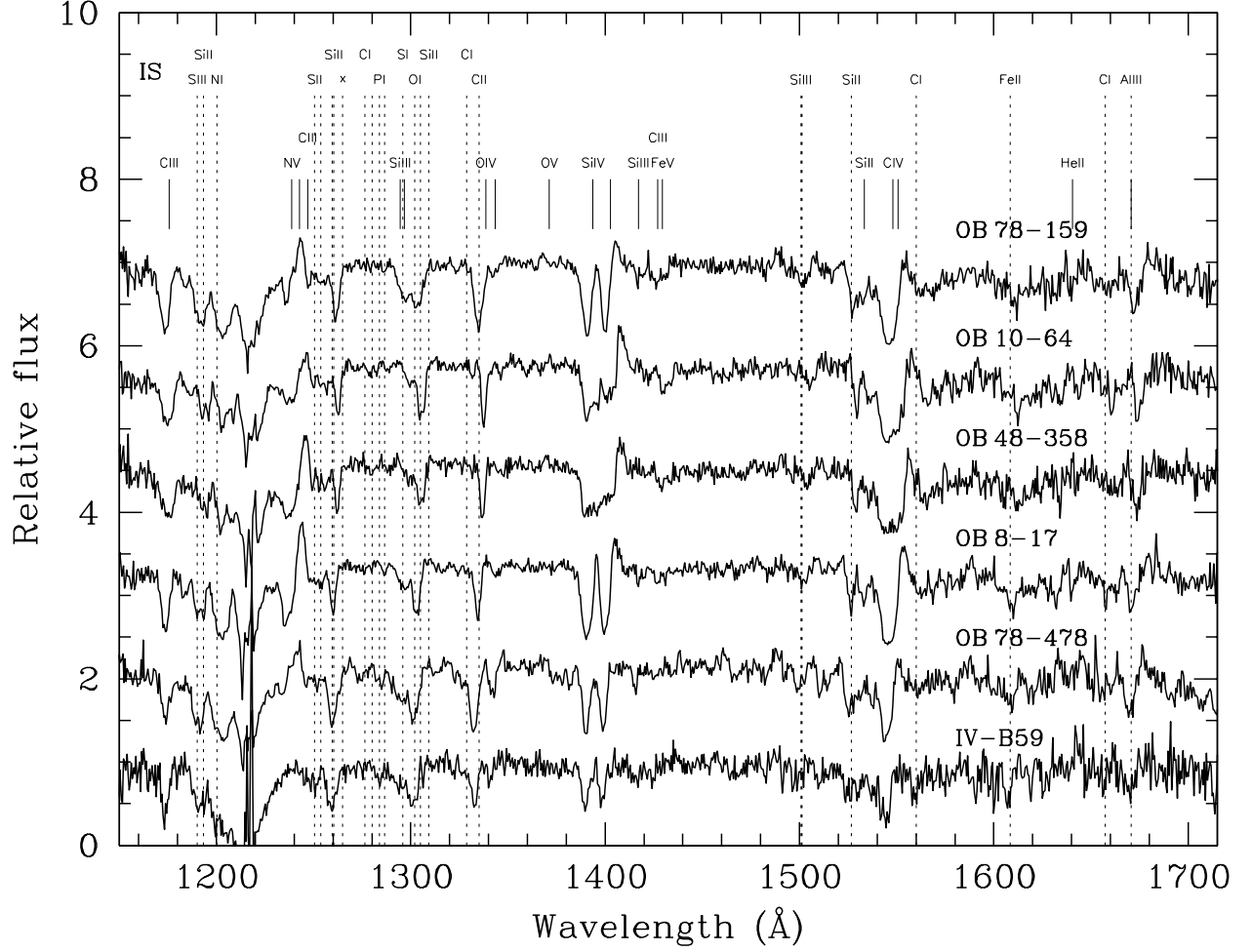


Fig. 1.— The rectified STIS spectra of the B supergiants observed in M31. A relative flux offset is applied for clarity. Identification for the main interstellar (dashed vertical lines) and stellar (vertical segments) features is provided.



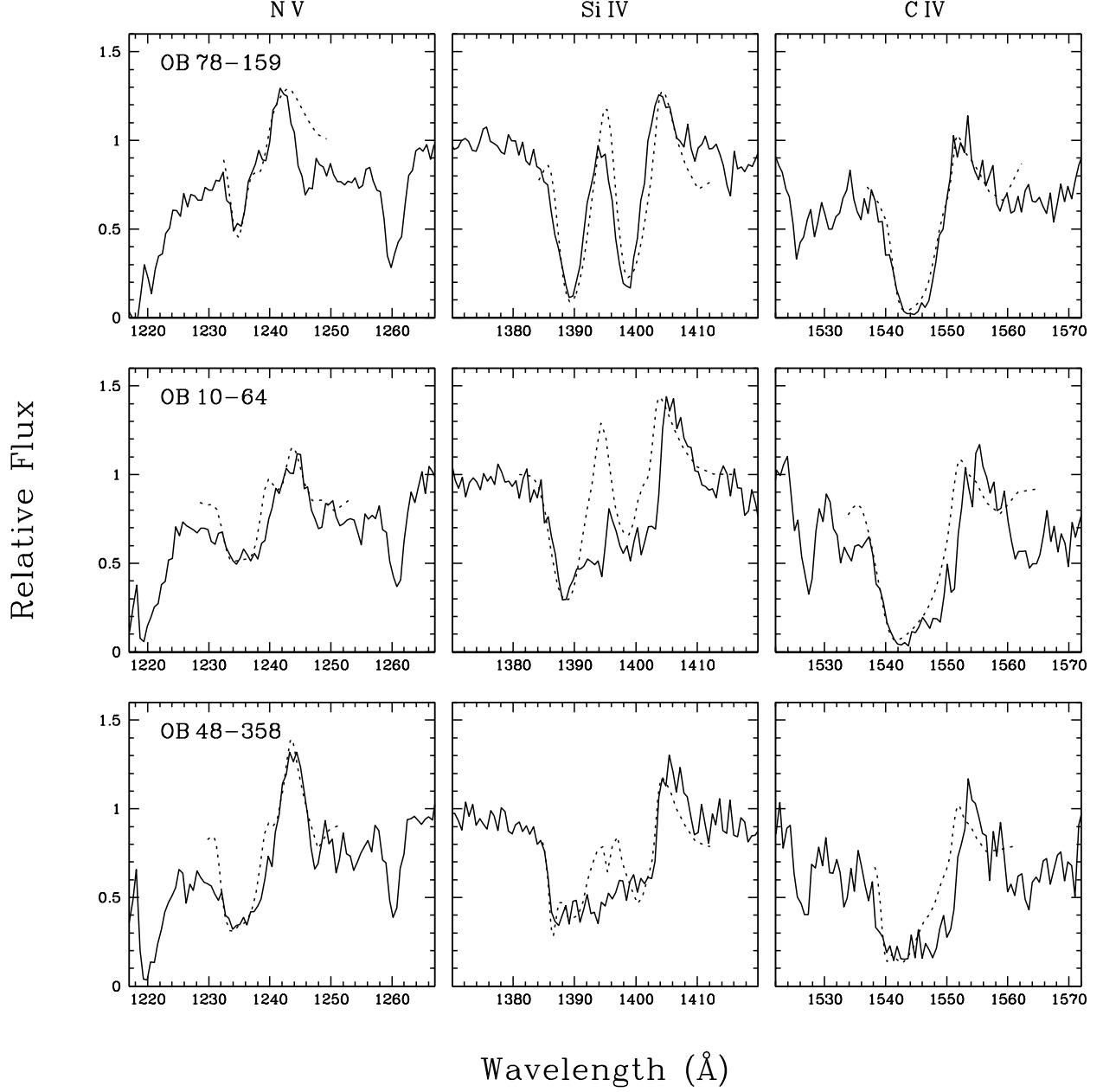


Fig. 2.— Profile fits to the N v  $\lambda$  1240, Si iv  $\lambda$  1400 and C iv  $\lambda$  1550 lines are shown as dotted lines superimposed on the observed normalized spectra, for the stars OB 78-159, OB 10-64 and OB 48-358.

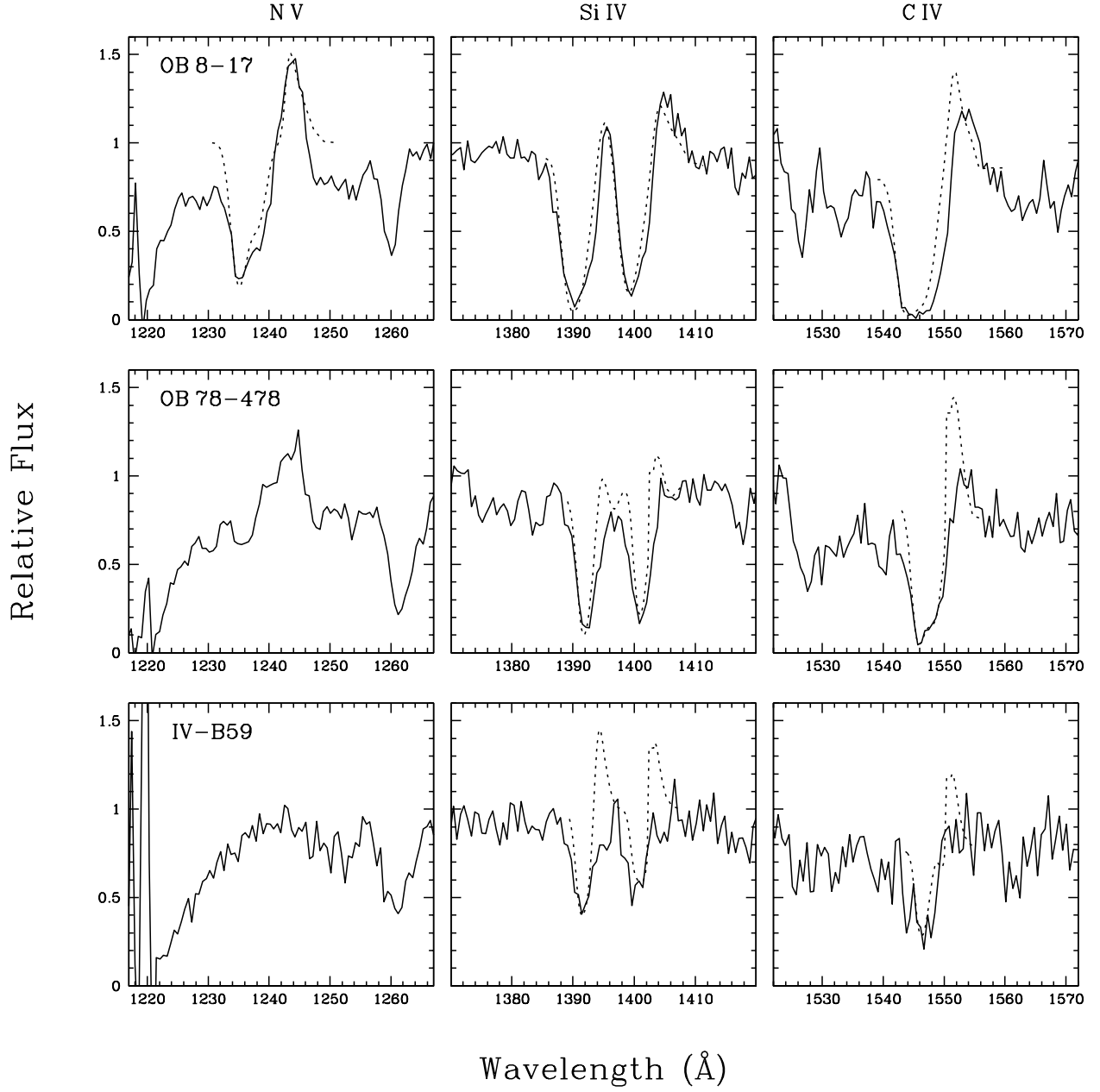


Fig. 3.— As Fig. 2, for stars OB 8-17, OB 78-478 and IV-B59.

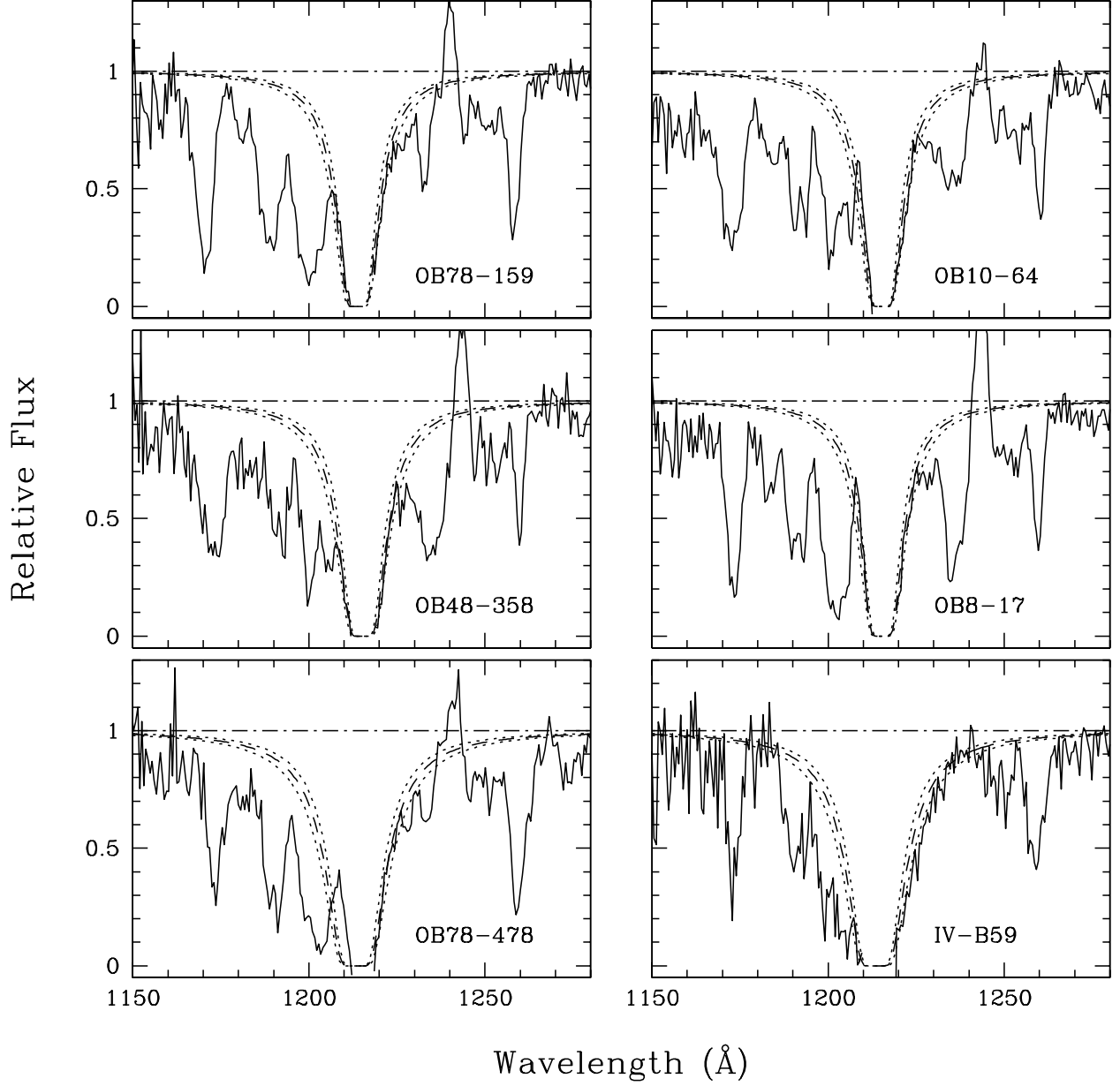


Fig. 4.— Fits to the interstellar Ly $\alpha$  absorption, assuming a pure damping profile, for the adopted neutral hydrogen column density (dashed line), and varying the column density by  $\pm 0.1$  dex (dotted lines).

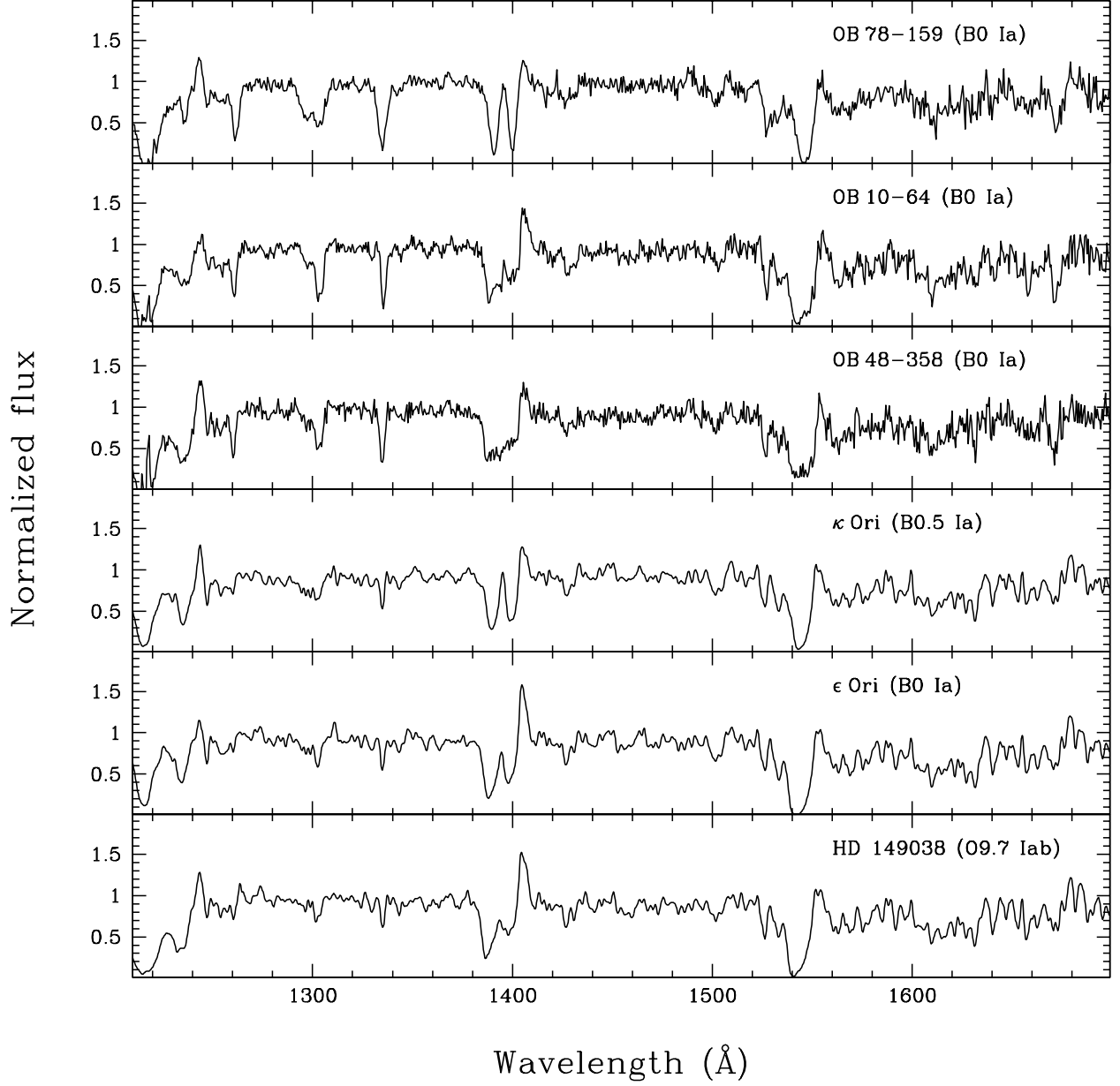


Fig. 5.— The STIS spectra of the three B0Ia stars in the M31 sample (upper three panels) are compared to IUE spectra of Galactic stars of similar spectral type, degraded to the resolution of the STIS spectra:  $\kappa$  Ori (B0.5Ia),  $\epsilon$  Ori (B0Ia) and HD 149038 (O9.7Iab) (lower three panels).

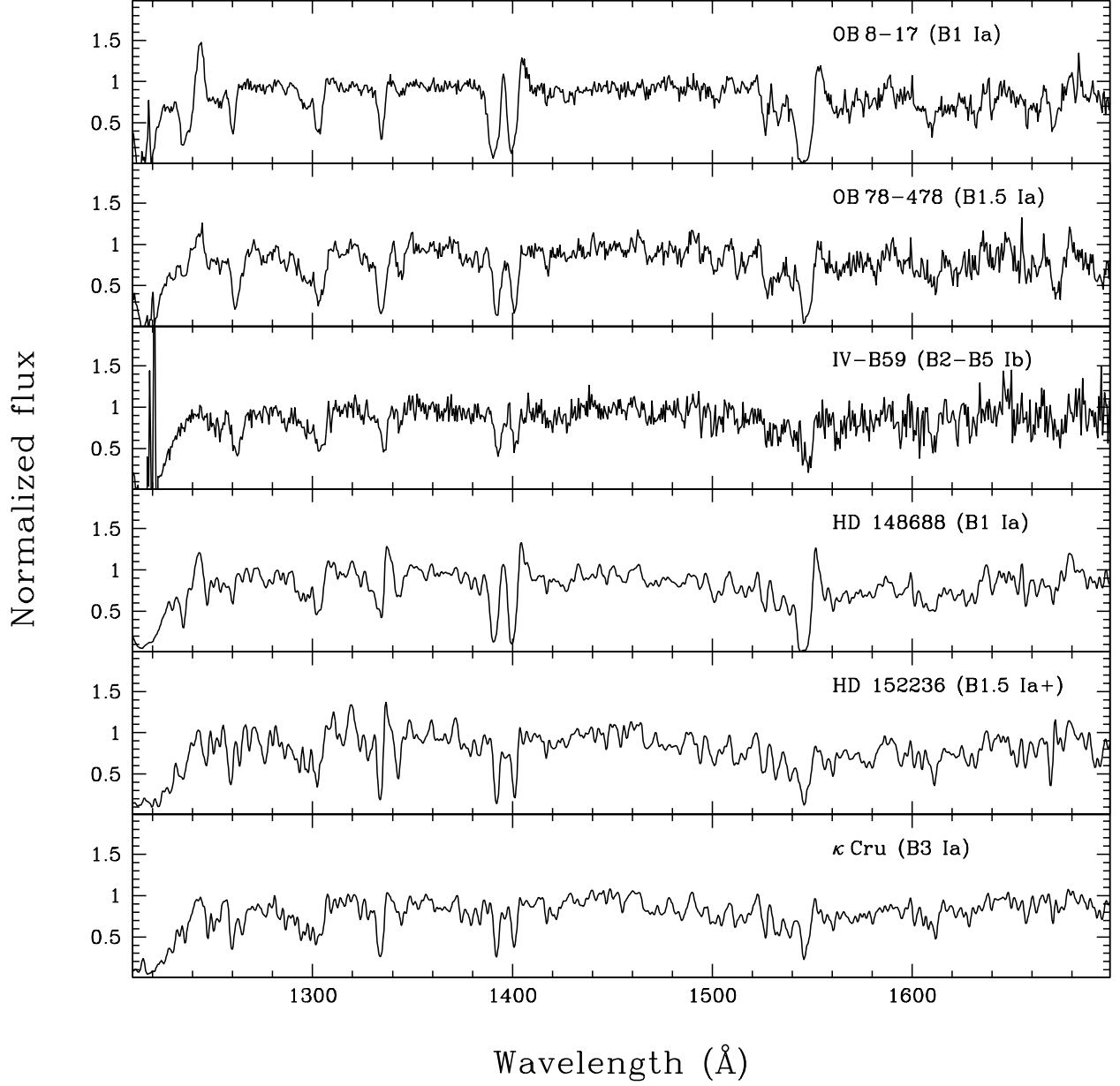


Fig. 6.— The three later-type supergiants in the M31 sample (upper three panels) are compared to IUE spectra of Galactic stars of similar spectral type, degraded to the resolution of the STIS spectra: HD 148688 (B1 Ia), HD 152236 (B1.5 Ia+), and  $\kappa$  Cru (B3 Ia) (lower three panels).

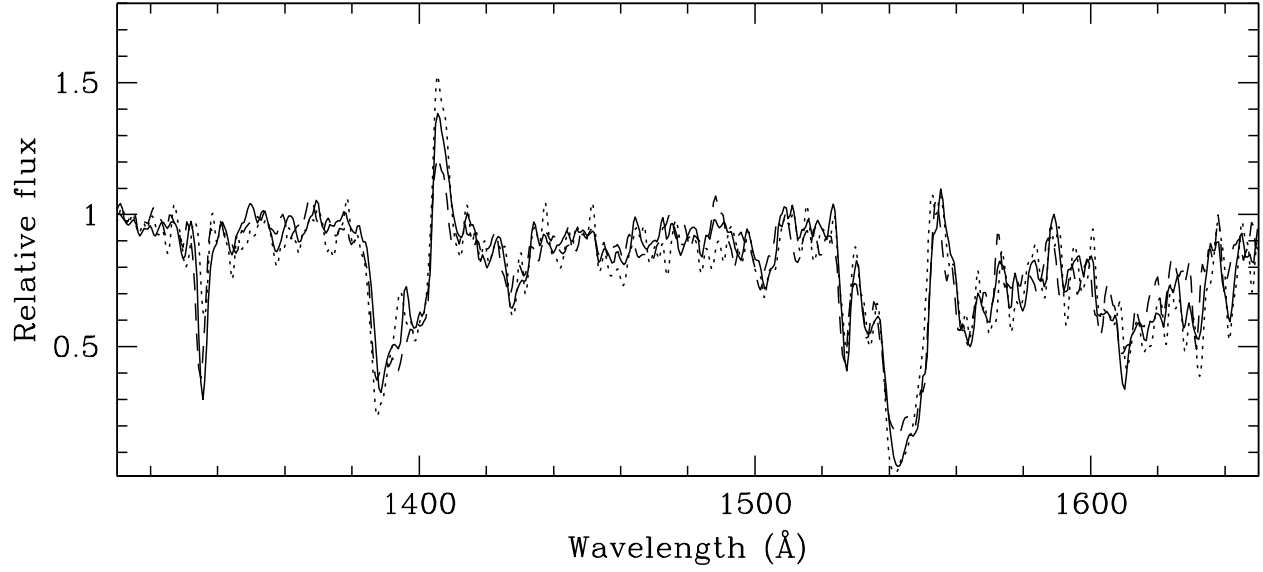


Fig. 7.— The spectra of the two M31 B0Ia supergiants OB 10-64 (full line) and OB 48-358 (dashed line) superimposed on the IUE spectrum of HD 149038 (O9.7Iab, dotted line).

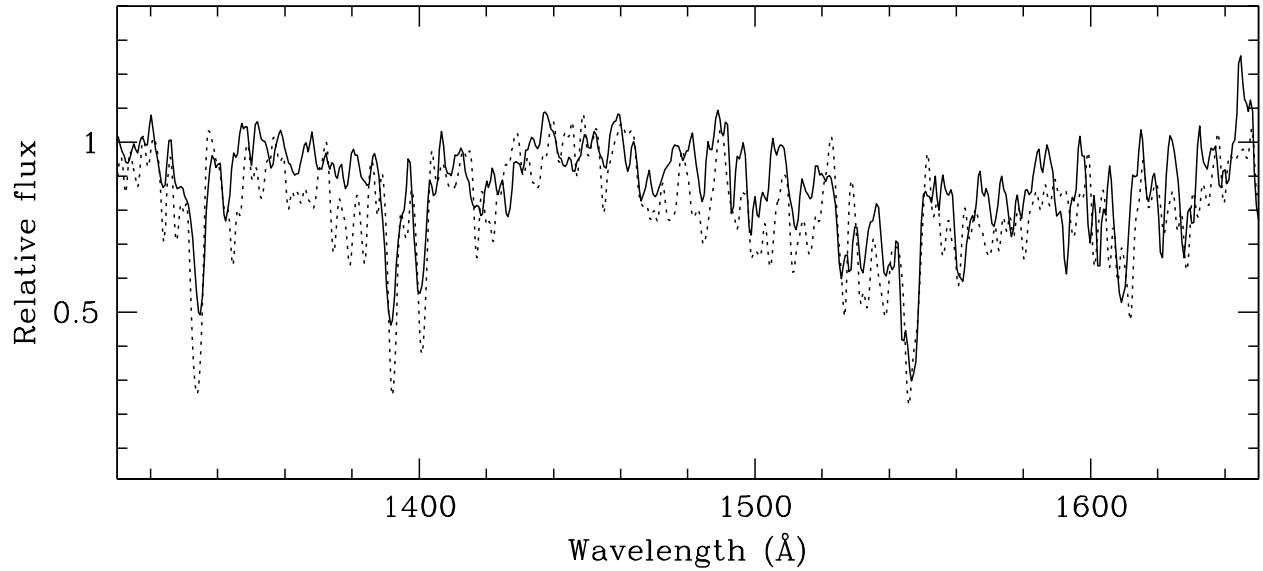


Fig. 8.— The spectrum of IV-B59 (full line) superimposed on the IUE spectrum of  $\kappa$  Cru (dotted line).

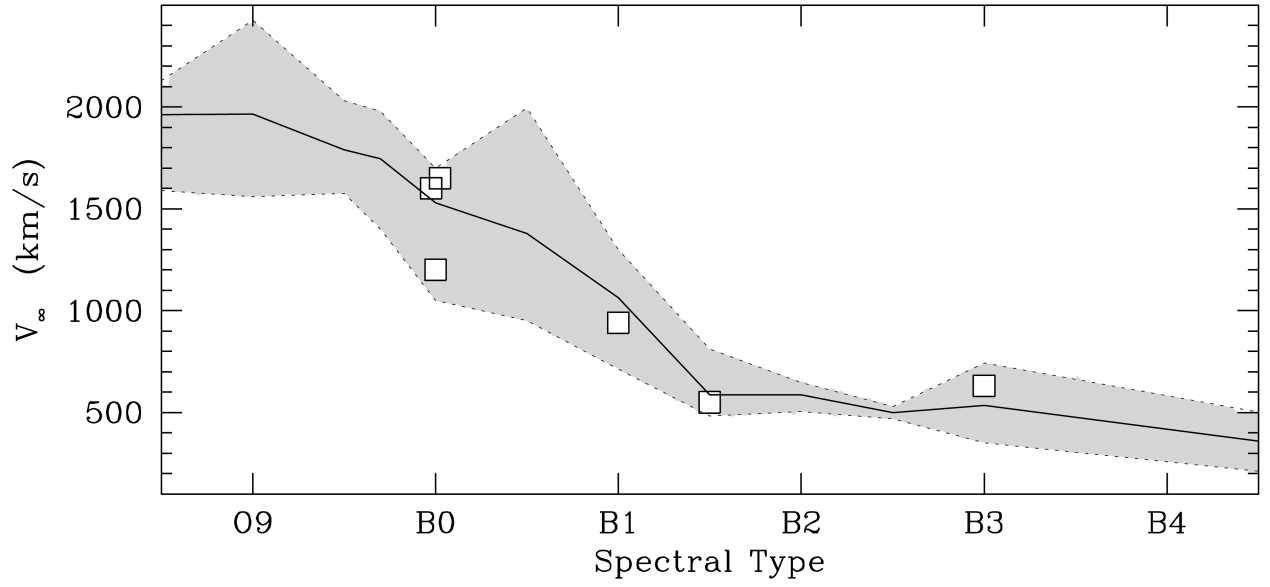


Fig. 9.— The terminal velocities as a function of spectral type for the M31 supergiants (open squares) are compared to the mean terminal velocities from the compilations of Haser (1995) and Howarth et al. (1997) (full line). The shaded area shows the range in terminal velocity for the Galactic stars. For star IV-B59 we have assumed a B3 type, given the present uncertainty in its spectral classification.

Table 1. STIS targets in M31

ID	R.A. (2000.0)	Decl. (2000.0)	$V$	$B - V$	Spectral Type		$v_{rad}$ ( $\text{km s}^{-1}$ )	Obs. date	Exp. time (sec)	Comments
					M95	T02				
OB 78-159	00 40 28.4	40 43 14.3	17.97	−0.05	B0 I	B0 Ia	−467	Feb 3, 1999	8223	composite
OB 10-64	00 44 10.4	41 33 16.2	18.10	−0.08	B1 I	B0 Ia	−113	Oct 1, 1999	8459	Smartt et al. (2000)
OB 48-358	00 45 13.2	41 39 38.4	18.70	−0.06	B0-1 I	B0 Ia	−107	Sep 29, 1999	14255	
OB 8-17	00 44 07.8	41 31 53.8	18.01	−0.06	O9-B1 I	B1 Ia	−102	Aug 9, 1999	8463	
OB 78-478	00 40 33.0	40 45 10.9	17.83	−0.10	B0-B1 Ib	B1.5 Ia	−561	Sep 26, 1999	5323	
IV-B59 <sup>a</sup>	00 37 33.3	40 00 36.7	17.60	0.00	B2 Iae <sup>b</sup>	B2 Ib-B5 Iab	−502	Jul 7-8, 2000	5323	

<sup>a</sup>Baade & Swope (1963)

<sup>b</sup>Humphreys (1979)

Table 2. Derived parameters

ID	R (Kpc)	12+ $\log(O/H)$ <sup>a</sup>	$E(B - V)$ <sup>b</sup>	$M_V$	$\log N(HI)$ ( $\text{cm}^{-2}$ )	$N(HI)/E(B - V)_0$ ( $10^{21} \text{cm}^{-2} \text{mag}^{-1}$ )	$v_\infty$ ( $\text{km s}^{-1}$ )	$v_{ta}$ ( $\text{km s}^{-1}$ )	$\beta$	$\log N$ ( $\text{cm}^{-2}$ )	
(1)	(2)	(3)	(4)	(5)	(6)	(7)	(8)	(9)	(10)	N v (11)	Si iv (12)
OB 78-159	9.5	...	0.14	−6.93	20.9	6.2 (4.0)	1200 (50)	150–350	0.8	15.24	15.34
OB 10-64	5.9	8.7	0.16	−6.86	20.9	4.9 (2.8)	1600 (100)	250–400	0.8	15.24	15.08 <sup>c</sup>
OB 48-358	11.6	8.7	0.23	−6.48	21.0	4.1 (1.8)	1650 (50)	100–250	0.7	15.58	15.42
OB 8-17	5.8	8.4	0.16	−6.95	20.9	4.9 (2.8)	940 (50)	200–300	0.7	15.59	15.59
OB 78-478	9.0	9.0	0.14	−7.07	21.2	16.0 (8.5)	550 (50)	80–250	0.7	...	15.42
IV-B59	21.8	...	0.14	−7.30	21.2	16.0 (8.5)	630 (100)	80–250	0.9	...	14.84 <sup>c</sup>

<sup>a</sup>Trundle et al. (2002)

<sup>b</sup>Massey et al. (1995); Humphreys (1979)

<sup>c</sup>No photospheric spectrum in fit